FSS-BASED ARTIFICIAL MAGNETIC CONDUCTOR FOR GAIN ENHANCEMENT OF DUAL-BAND CPW-FED SPLIT RING ANTENNA

Sujit Goswami[1], *Sujit Kumar Mandal[2], Soumen Banerjee[3], Ayan Chatterjee[4]

[1]*Department of Electronics and Communication Engineering, Asansol Engineering College, Asansol, West Bengal, India,* [1]*sujit.ece@aecwb.edu.in*
[2]*Department of Electronics and Communication Engineering, National Institute of Technology, Durgapur, West Bengal, India,* [2] *skmandal.ece@nitdgp.ac.in*
[3]*Department of Electronics and Communication Engineering, Narula Institute of Technology, Agarpara, Kolkata, West Bengal, India,* [3]*hello.sbanerjee@gmail.com*
[4]*Department of Electronics and Communication Engineering, Institute of Engineering and Management, University of Engineering and Management, Kolkata,* [4]*ayanmrinal26@gmail.com*

Abstract: This paper presents the development of a novel low profile dual-band co-planar waveguide (CPW)-fed split ring-shaped antenna with improved radiation performance in the broadside direction using a frequency selective surface (FSS)-based artificial magnetic conductor (AMC). The CPW-fed split ring antenna is developed to operate at the two operating bands with the center frequencies of 2.4 GHz and 5.8 GHz, having bi-directional radiation characteristics. The FSS-based AMC is designed with the reflection phase close to 0° for the corresponding resonating frequencies of both the working bands of the antenna. The proposed AMC is introduced as a substrate at a relatively lower spacing of λ/12, which is much less than the quarter-wavelength spacing as used in the conventional approach for enhancing antenna gain at the broadside direction. By embedding the FSS-based AMC layer, the antenna exhibits the highest gain of 8.5 dBi and 8.92 dBi in the lower and upper bands, respectively.

Keywords: Dual-band, microstrip antenna, CPW-fed, FSS, AMC.

1. INTRODUCTION

In recent years, multi-band and wideband operations embedding frequency selective surface (FSS) in patch antennas have become a growing global interest amongst researchers. A suitable combination of the printed antenna and a reflective surface, like FSS, results in overcoming the limitation of lower antenna gain and directivity. FSS is a periodic structure comprising a one-dimensional or two-dimensional lattice of specific geometries or slots under metallic screens, which acts as an analogue spatial filter. The artificial magnetic conductor (AMC) is characterized by the reflection coefficient with zero phase for the frequency range under consideration.

Many FSS-Antennas with composite structural design generating higher gain have been reported in the literature. An FSS-based compact dual-band antenna with dual polarized and improved gain comprising a lower band and higher band antenna elements is demonstrated in [1]. To reduce the total antenna size, the higher band antenna element is positioned just underneath a dual-layer FSS-based lower band radiator. The lower band FSS-based radiator is made so that it passes the higher band. As a result, the radiation from the higher band underneath the element can pass through the lower band radiator. Elsewhere, several FSS-based metaheuristics, multi-layer techniques have been introduced to achieve multiband and wide-band antennas [2 - 9].

The antenna performance with FSS depends on the shape of the slots, lattice geometry, as well as the electrical characteristics of the substrate. A dual band FSS consisting of regular Jerusalem cross-shaped elements is applied for improved antenna performance, such as gain, bandwidth, and return losses [10]. A method with a double layered, low-profile, band-stop FSS is proposed for gain improvement of a conventional wide-slot antenna in [11]. The gain enhancement of a compact pentagon-shaped slot-loaded wideband antenna with offset feed using a reflective frequency-selective surface to cover 3 - 6 GHz application is proposed in [12]. An FSS based embedded broadband, high gain miniaturized microstrip antenna is reported in [13]. Here, the multiband response is attained by using an 'N' shaped metallic patch surface and the 'I' shaped ground plane. The broadband characteristics is accomplished with perfect impedance matching with modified feeding mechanism and a single step matching staircase architecture. FSS is also deployed to realize circular polarization with improved antenna gain [14].

The properly designed FSSs have a wide area of filtering operation in electromagnetic (EM) field, which includes WLAN, 5G mobile, and ISM band [15 - 18] applications. In wideband FSSs, introducing an air gap between the layers reduces mutual coupling and thereby enhances reflection performance across a broader bandwidth. In general, multiple FSS layers are cascaded to achieve ultra-wideband [19, 20] and X-band response in [21]. Customarily, the transmission and reflection characteristics of an FSS are influenced by the shape, size, periodicity, and overall geometry of its elements. The common FSS geometries include monopoles, dipoles, square loops, fractal patterns, and other specialized structures. Cascading multiple FSS layers is a communal approach to enhance gain and achieve dual band response in microstrip antennas [22 - 25]. It is to be mentioned that one notable application involves using an AMC structure as the substrate for a low-profile conformal antenna.

By aligning the antenna's resonant frequency with that of the AMC, antenna performance can be enhanced while simultaneously suppressing surface wave propagation within the substrate [26, 27]. A novel approach employing an AMC is proposed to realize an edge-fed, wideband, high-gain patch antenna in [26]. The multiband characteristics of a conventional electromagnetic band-gap (EBG) AMC, implemented above a perfect electric conductor (PEC) backplane, is investigated in [27]. Two planar FSSs with distinct configurations, along with a monopole antenna that exhibits a dual-band response is presented in [28]. A dual-band, compact monopole antenna with enhanced gain has been designed using a frequency selective surface in [29]. A printed monopole antenna with high gain and dual-band characteristics is presented for applications in wireless local area networks (WLAN) and Internet of Things (IoT) sensor networks in [30]. Another compact pattern-reconfigurable antenna based on the tunable gap-incorporated band-stop FSS unit cell is presented for various wireless communication systems [31]. A compact broadband Y-shaped monopole antenna with band-notched characteristics is reported for WLAN and WiMAX applications [32]. A wideband and high-selectivity amplifying frequency selective surface (AFSS) has been proposed in [33]. Compared to the other FSS available, AFSS can increase the amplitude of electromagnetic waves within the pass-band with relative amplification bandwidth of 30%. A wideband, high-gain planar trapezoidal monopole antenna utilizing a single-layer FSS is proposed in [34]. FSS is also used to design a miniaturized broadband planar antenna with better impedance matching and higher gain for modern communication systems in [35].

Usually, to improve the radiation characteristics of the designed antenna, FSS is employed as a reflecting radiator for the operating band under consideration, and a suitable gap is introduced between the radiating patch and the FSS layer. Introduction of such a gap increases the overall antenna size. In this paper, a novel FSS-based AMC is reported to design a low-profile antenna with improved performances and dual-band characteristics. By employing the FSS-based AMC layer, the radiation of a CPW-fed monopole antenna is enhanced along the broadside direction. The presented antenna results in a high gain of 8.5 dBi and 8.92 dBi for the operating bands of 2.4 GHz and 5.8 GHz, respectively. The proposed design implements an AMC-based periodic structure as a substrate below the CPW-fed antenna for its gain enhancement. Unlike conventional reflective periodic structures such as frequency selective surfaces, that requires quarter wavelength ($\lambda_0/4$) spacing between antenna and the reflector with the AMC used here is placed at a spacing of 8 mm that is on the order of $\lambda_0/15$. In comparison to the existing similar works [36 - 38], the proposed design achieves smaller profile due to the choice of proper unit cell phase response.

Moreover, more gain enhancement of 4-7 dBi is achieved in comparison to 1.5 dBi in [36]. The detailed design steps, antenna analysis, and simulated results, along with the experimentally measured data, are presented in the remaining paper.

2. DESIGN OF THE CPW-FED SPLIT RING-SHAPED ANTENNA

A monopole antenna with CPW-fed as shown in Fig. 1 is chosen as the reference antenna for the proposed design. The CPW feeding is used for low dispersion, broadband performance, ease of integration with the front ends of wireless communication systems and cost-effectiveness due to one-sided fabrication. Compared to narrowband (2-5%) patch antennas, monopole antenna is preferred for its controllable wide as well as multi-band response. The referred antenna architecture along with its various dimensions is indicated in Fig. 1(a). The feeding network to excite the antenna is obtained via the conventional equations as detailed in [39]. On the other hand, the split ring-shaped quarter-wave monopole antenna parameters are tuned to as to operate at both the 2.4 GHz as well as 5.8 GHz bands.

Different antenna design parameters with their respective dimensions are summarized in Table 1. The length of the modified U-shaped monopole is computed by the equation (1) evolved using the concepts as detailed in Chapter 07, [39] and Chapter 08, [40]:

$$L_r = \frac{c_0}{4 \times f_1 \times \sqrt{(\varepsilon_r + 1)/2}}\,. \quad (1)$$

The designed antenna is reproduced on FR4 substrate characterized by height 0.8 mm, relative permittivity 4.4 with loss tangent 0.02. The strip width W_r is chosen as 2 mm such that the strip equivalent inductance provides the required resonating frequency. Since, the larger (smaller) strip width leads to a decrease (increase) equivalent inductance and would increase (decrease) the resonating frequency. The ring gap g_a is chosen so as to tune the resonating frequencies at the desired values. The corresponding antenna prototype is illustrated in Fig. 1(b). The CPW feedline width W_c and the gap W_g, both are calculated using conventional design equations as detailed in [39]. The surface current distribution performance at 2.4 GHz and 5.8 GHz is presented in Fig. 2 that illustrates the flow of current and determines the corresponding resonating frequency. Different applications such as bidirectional (both front and back side) radiation in the orthogonal plane of the antenna need to be tailored to unidirectional pattern. Specifically for body area network, vehicular communication, ground penetrating radar, etc. the antenna should radiate primarily in the broadside direction over an adequate bandwidth. In this regard, a grounded FSS structures is proposed to achieve the desired radiation characteristics with improved performances. Design of the FSS-based AMC and the performances of the antenna with its introduction are discussed in the following subsequent sections.

3. DESIGN AND ANALYSIS OF THE FSS-BASED AMC

The 3-D aspect of the presented antenna and FSS-based AMC placed below the antenna is presented in Fig. 3. The array of unit cell under the FSS provides AMC characteristics that are depicted in Fig. 4(a). The FSS array cell consisting a plus-shape (+) metal strip having stub at each ends and a square loop strip surrounding it. While the stubbed plus-shaped FSS is tuned to resonate at 5.8 GHz, the outer side square loop is employed to have the potential feature of AMC at 2.4 GHz. The length of the square loop is determined at the desired resonating frequency f_1 = 2.4 GHz using (2) as detailed in Chapter 02, [41].

$$L_p = \frac{c_0}{6\times f_1\times\sqrt{(\varepsilon_r+1)/2}} \quad (2).$$

The length of inner cross L_a is determined as (3) to obtain resonance at 5.8 GHz as detailed in Chapter 02, [41].

$$L_a = \frac{c_0}{3.5\times f_2\times\sqrt{(\varepsilon_r+1)/2}} \quad (3)$$

Here the resonating frequency f_2 is chosen as 5.8 GHz and the length is fine-tuned followed by the calculation using (3) because of the increased spacing between cross elements of consecutive cells and inclusion of ground plane below the periodic structure. The stub length L_s is changed for fine tuning the desired operating frequency. The unit cell dimensions are listed in Table 2. The obtained dimension (13.2 mm×13.2 mm) of unit cell is of the order of 0.1λ_0 with reference to the operating frequency 2.4 GHz. Finally, a ground plane is introduced on the reverse side of the chosen FR4 substrate with height t = 1.6 mm.

The FSS-based AMC prototype is shown in Fig. 4(c). Without ground plane, the FSS exhibits reflection at operating frequency, however provides a sharp change in reflection phase between ±180° and, when it is placed below the antenna with spacing less than quarter wavelength, it causes destructive interference of the radiated waves resulting in 180° phase shift. The proposed FSS-based AMC is parametrically analyzed using ANSYS HFSS v19.0. The simulation setup of the

AMC is depicted in the Fig. 4(b). The AMC unit cell is designed above the substrate with the ground plane below. The metallic patch and ground plane are realized by assigning them with finite conductivity. The unit cell is surrounded by a vacuum cubical box to realize the infinite array of the unit cells with periodicity as mentioned in Table 2. Two opposite faces of the simulation box are assigned as perfect electric (Perfect E) boundaries, while the remaining two opposite faces are designated as perfect magnetic (Perfect H) boundaries. This setup is required for infinite array of the unit cell. The top and bottom faces are designated as wave ports to serve as the excitation and output interfaces. An integration line is drawn between two perfect E *w*alls. The simulation is performed over the 2-7 GHz band and the S-parameters are observed. Keeping other dimensions of the unit cell at constant values, for different stub lengths the changes in reflection phase response are depicted in Fig 5. It can be illustrated that changes in the stub length dominantly affects the higher operating frequency and with increasing stub-length, the higher operating frequency giving zero phase reflection decreases (shift towards left). However, the lower operating frequency exhibiting zero reflection phases at 2.4 GHz does not affect significantly. The reflection phase variation with the variation in loop dimension is presented in Fig. 6. It is noted that with change in loop dimension, the band at 2.4 GHz is shifted whereas the frequency band at 5.8 GHz does not shift significantly. This is because, the increase in stub-length leads to increase the capacitance between consecutive unit cell which results in to reduce the corresponding resonating frequency. For different loop dimension, the reflection phase characteristic is presented in Fig 6. It can also be seen that the variations in the loop dimension substantially changes the lower operating band at 2.4 GHz but the higher operating band at 5.8 GHz not so considerably affected. The FSS-based AMC is adjusted to maintain the reflection phase of 0° with a variation between ±90° with respect to the desired operating frequency bands at 2.4 GHz and 5.8 GHz respectively. Thus, the proposed FSS-based AMC

exhibits a reflection coefficient close to 0 dB with no transmission due to metallic ground plane.

4. CHARACTERISTICS OF THE ANTENNA WITH FSS-BASED AMC

To observe the outcome of the proposed FSS-based AMC on the performance of antenna, it is located below the CPW-fed split ring-shaped antenna with a spacing of *H*, which is smaller than the quarter wavelength of the lower operating band at 2.4 GHz. This dual-band AMC is incorporated for antenna radiation enhancement in the broadside direction for both the frequency bands. The antenna is fabricated with the AMC as presented in Fig. 7. The antenna characteristics are investigated with and without the FSS-based AMC. Considering the reflection phase close to zero in both the operating bands, the FSS-based AMC can be placed very close to the antenna to reduce back radiation leading to enhanced gain in the opposite direction.

Simulated antenna return loss (S_{11}) with and without the FSS based AMC at H = 10 mm are shown in Fig. 8. It can be followed that by use of FSS-based AMC, where the operating bands at 2.4 GHz and 5.8 GHz do not shift significantly. However due to loading effect of high surface (FSS), two resonances can be observed in the higher band. The measured result is also included in the same graph that exhibits good mapping between the simulated and the measured results of S_{11}. The spacing between antenna and AMC, '*H*' is varied to achieve adequate impedance matching and reflection coefficient over the complete frequency band. The reflection coefficients (S_{11}) of antenna with FSS and without FSS are presented in Fig. 9 for set of values of '*H*'. With increase in '*H*' value, the impedance matching gets improved near 2.4 GHz, however the same does not change significantly in the upper band at 5.8 GHz. Rather at H= 12 mm the impedance matching gets degraded in the upper band at first resonance of 5.5 GHz and in the middle of the band. Thus it can be noted that for a spacing of H = 10 mm, the antenna exhibits adequate impedance matching and the reflection below 10 dB in both the bands. The antenna with AMC exhibits -10 dB bandwidth of 25% in lower band with 2.35 GHz resonance and bandwidth of 18% in upper band with resonances at 5.5 GHz and 5.93 GHz respectively. With the FSS-based AMC the second resonance near 5.9 GHz occurs possibly due to the fact that, the FSS exhibits reactive impedance (inductive/capacitive) which compensates the reactive impedance of opposite nature (capacitive or inductive) of the antenna leading to a near zero imaginary part of the antenna input impedance.

The antenna radiation characteristics with AMC are studied in far field. Simulated radiation patterns at φ= 90° and φ= 0° planes, are shown in Fig. 10 for 2.35 GHz and in Fig. 11 for 5.5 GHz. At both the frequencies, the back radiation is significantly reduced by around 8 - 10 dB, with the implementation of FSS-based AMC as per the front-to-back (F/B) ratios included in Table 3. With minimization in back radiation, the broadside antenna gain is improved for the required frequency range and values are listed in Table 3 along with the front-to-back ratio (F/B). As evident, the antenna gain is enhanced up to 8.5 dBi at 2.35 GHz whereas the enhancement is up to 8.92 dBi at 5.5 GHz. The measurement setup for the radiation pattern and gain is depicted in Fig. 12. Here, the antenna gain is measured using gain-transfer method. In this mechanism, the standard gain (reference gain) is utilized in order to estimate the absolute gains. Initially, relative gain measurements are performed, and by comparing these with the known gain of a standard reference antenna, absolute gain values are obtained. At first, the antenna-AMC under test is used as the receiving antenna, and the received power (P_T) into a matched load is measured. Then the test antenna is replaced with a standard gain antenna, and the received power (P_S) is measured under identical conditions. In both cases, the geometrical setup and input power are kept constant.The gain in the far field region is calculated using equation (4)

$$(G_T)_{dB} = (G_S)_{dB} + 10 \log_{10} (P_T / P_S) \qquad (4)$$

where $(G_T)_{dB}$ and $(G_S)_{dB}$ are the gains (in dB) of the test antenna and standard gain antennas. The return loss of the fabricated prototype is measured using an Agilent vector network analyzer (VNA), while its radiation pattern is evaluated using the gain transfer method. The measurement setup includes a Hittite HMC-T2100 microwave signal generator (10 – 20 GHz), a Krytar 9000B power meter, and a standard gain horn antenna.

The measured F/B ratio and peak antenna gain with AMC are also listed in the Table 3 that is in well agreement with the simulated values.

Three-dimensional gain plots of antenna with and without the FSS-based AMC as well as the antenna backed by metallic reflector are shown in Fig. 13, Fig. 14 and Fig. 15 for 2.35 GHz and 5.5 GHz respectively. The plots confirm significant reduction in back radiation and enhancement in broadside gain of the CPW-fed split ring shaped antenna with the use of FSS-based AMC.

A comparative study of the effect of AMC substrate and metallic reflector on the performance of the antenna is carried out for better understanding the role of AMC. The antenna is backed by a continuous metallic ground plane by replacing the AMC. The reflection coefficient is plotted in the Fig. 8 along with other combinations. It can be observed that the antenna backed by metallic ground exhibits almost similar resonating frequencies at 2.04 GHz and 5.75 GHz. The lower frequency of resonance is shifted slightly. However, there is a significant difference in the radiation characteristics of the antenna backed by metal. As shown in the Fig. 15 the antenna backed by continuous metallic ground shows a peak gain of 1.8 dBi at 2.04 GHz which is much less than the antenna in the lower operating band. The gain however at 5.75 GHz in the upper band 9.4 dBi that is more is compared to the antenna backed by the FSS based AMC. This justifies the fact that the purpose of antenna gain enhancement over multiple bands cannot be served by a continuous metallic plane in place of AMC. This is because AMC provides nearly zero reflection phase at the operating frequencies, whereas ground plane offers 180-degree phase shift at both the frequencies and in such case radiation enhancement requires height variation. In a single antenna structure different heights at different frequencies cannot be maintained.

5. PERFORMANCE ANALYSIS AND COMPARATIVE STUDY

A comparative study of the performance characteristics of the proposed antenna with respect to other similar types of antennas are presented in Table 4. It is evident that the proposed design is compact and provides a wider bandwidth compared to the structure in [18], while utilizing two layers of FSS unlike the single-layer approach in [13]. The proposed FSS demonstrates superior angular stability compared to [13], despite being polarization-dependent, and offers a lower profile in terms of interlayer spacing when compared to the design in [18]. In terms of the gain performance, the proposed antenna shows improved gain in comparison to both design [13] and [18]. The novelty of the proposed FSS lies in its compact size ($0.1\lambda_0 \times 0.1\lambda_0$ at the center frequency), low profile ($0.1\lambda_0$), enhanced angular stability up to 90°, and its nearly linear reflection phase variation across the desired frequency band.

6. CONCLUSION

The enhancement of radiation characteristics and impedance of a dual band CPW-fed split ring shaped monopole antenna operating at 2.4 GHz and 5.8 GHz is studied with the implementation of a dual-band FSS-based AMC array. With the inclusion of the FSS-based AMC, the broadside antenna gain is improved by 4-7 dBi by reducing the antenna back radiation while the antenna impedance bandwidth and resonance frequencies are almost remained same at both the operating bands. In the two bands, the back radiation is reduced by around 7-10 dBi. The introduction of AMC includes a second resonance with antenna reflection coefficient and improved impedance matching. The spacing between the antenna and FSS is preserved at 10 mm which is less compared to the conventional quarter wavelength value at the center frequency (2.35 GHz) of the lower band. The proposed design is useful for improving the antenna gain with multiband characteristics.

Acknowledgement

This work is financially supported by the Ministry of Electronics and Information Technology (MeitY), Govt of India, under the Visvesvaraya Ph.D. scheme (Grant No. Ph.D.-MLA-4(29)/ 2015-16).

REFERENCES

[1] Yang, S. J. and Zhang, X. Y. "Frequency Selective Surface-Based Dual-Band Dual-Polarized High-Gain Antenna", *IEEE Transactions on Antennas and Propagation*, vol. 70, Issue. 30, 2022. DOI: 10.1109/TAP.2021.3111222.

[2] Mondal, R., Reddy, P. S., Sarkar, S., Sarkar, D. C. and Sarkar, P. P. "Wideband to narrowband/dual band characteristics of monopole antenna using frequency selective surfaces", *International Journal of Communication Systems*, vol. 26, 2022. DOI: 10.1002/dac.5430.

[3] Braz, E. C. and Compos, A. "Dual/ Wideband Multifractal Frequency Selective Surface for Applications in S and X-Band", *Microwave and Optical Technology Letters*, vol. 56, Issue. 10, pp. 2017-2022, 2014. DOI: 10.1002/mop.28561.

[4] Kundu, S. and Chatterjee, A. " A compact super wideband antenna with stable and improved radiation using super wideband frequency selective surface", *AEU - International Journal of Electronics and Communications*, 150, 154200, 2022. DOI:10.1016/ j. aeue.2022.154200.

[5] Kushwaha, N. and Kumar, R. "*Design of a Wideband High Gain Antenna Using FSS for Circularly Polarized Applications*." *AEU-International Journal of Electronics and Communications*, vol. 70, Issue. 9, pp. 1156-1163, 2016, DOI:10.1016/j.aeue. 2016.05.013.

[6] Xie, D., Liu, X., Guo, H., Yang, X., Liu, C. and Zhu, L. "A Wideband Absorber with a Multi-Resonant Gridded-Square FSS for Antenna RCS Reduction." *IEEE Antennas and Wireless Propagation Letters*, vol. 16, pp. 629-632, 2017. DOI: 10.1109/LAWP. 2016.2594213.

[7] Lins, H. W. C., Barreto, E. L. F. andd'Assunção, A. G. "Enhanced Wideband Performance of Coupled Frequency Selective Surfaces Using Metaheuristics." *Microwave and Optical Technology Letters*, vol. 55, Issue.4, pp. 711-715, 2013. DOI: 10.1002/mop.27451.

[8] Chatterjee, A. and Parui, S. K. "A Dual Layer Frequency Selective Surface Reflector for Wideband Applications", *Radioengineering*, vol. 25, Issue 1, pp. 67-72, 2016, DOI: 10.13164/ re.2016. 0067.

[9] Maity, S., Tewary, T., Mukherjee, S., Roy, A., Sarkar P. P. and Bhunia, S. "Wideband hybrid microstrip patch antenna and gain improvement using frequency selective surface", *International Journal of Communication Systems*, vol. 35, Issue. 14, 2022, DOI: 10.1002/dac.5268.

[10] Chen, H. Y. and Tao, Y. "Performance Improvement of a U-Slot Patch Antenna Using a Dual-Band Frequency Selective Surface with Modified Jerusalem Cross Elements." *IEEE Transactions on Antennas and Propagation*", vol. 59, Issue.9, pp. 3482-3486, 2011. DOI: 10.1109/ TAP.2011.2161440.

[11] Chatterjee, A. and Parui, S. K. "Gain Enhancement of a Wide-Slot Antenna Using Dual-Layer, Bandstop Frequency Selective Surface as a Substrate." *Microwave and Optical Technology Letters*, vol. 57, Issue. 9, pp.2016-2020, 2015. DOI: 10.1002/mop.29250.

[12] Chatterjee, A. and Parui, S. K. "A Compact Wideband Frequency Selective Surface for Gain Enhancement of a Wide-Slot Antenna." *In International Symposium on Antennas and Propagation (APSURSI), IEEE*, pp. 357-358, 2016, DOI: 10.1109/APS.2016.7695887.

[13] Tewary, T., Maity, S., Mukherjee, S., Roy, A., Sarkar, P. P. and Bhunia, S. "FSS embedded high gain 'N' shaped miniaturized broadband antenna", *AEU - International Journal of Electronics and Communications*, vol. 58, 154465, 2023. DOI:10.1016/j.aeue.2022.154465.

[14] Guthi, S. and Damera, V. "High gain and wideband circularly polarized S-shaped patch antenna with reactive impedance surface and frequency-selective surface configuration for Wi-Fi and Wi-Max applications", *International Journal of RF and Microwave Computer-Aided Engineering*, vol. 31, Issue. 11, 2021. DOI: 10.1002/mmce.22865.

[15] Natarajan, R., Kanagasabai, M., Baisakhiya, S., Sivasamy, R., Palaniswamy, S. and Pakkathillam. J. K. "A Compact Frequency Selective Surface with Stable Response for WLAN Applications." *IEEE Antennas and Wireless Propagation Letters*, vol.12, pp. 718-720, 2013, DOI: 10.1109/LAWP. 2013.2264837.

[16] Chengming, S., Zou, J., Gao, J. and Liu, C. "Gain Enhancement of a Dual-Band Antenna with the FSS." *Electronics*, vol. 11, Issue, (18) 2882, 2022, DOI: 10.3390/ electronics11182882.

[17] Decoster, B., Maes, S., Cuiñas, I., Sánchez, M. G., Caldeirinha, R. and Verhaevert, J. "Dual-Band Single-Layer Fractal Frequency Selective Surface for 5G Applications", *Electronics*, 10, 2880, 2021, DOI: 10.3390/electronics10222880.

[18] Fernandes, E. M., Farias, M. W. B., da Silva, L., da S. Briggs, A. L. P., de S. Campos, de Araújo, H. X., Casella, I. R. S., Capovilla, C. E., Souza, V. P. R. M. and Matos, L. J. de "2.4–5.8 GHz dual-band patch antenna with FSS reflector for radiation parameters enhancement." *AEU - International Journal of Electronics and Communications*, vol. 108, pp. 235-241, 2019, DOI: 10.1016/j.aeue.2019.06.021.

[19] Adibi, S., Honarvar M. A., and Lalbakhsh, A. "Gain Enhancement of Wideband Circularly Polarized UWB Antenna Using FSS, *Radio Science*, vol. 56, Issue.1, 2020, DOI: 10.1029/ 2020RS007098.

[20] Das, P., and Mandal, K. "Modelling of ultra-wide stop-band frequency-selective surface to enhance the gain of a UWB antenna", *IET Microwaves, Antennas & Propagation*, vol. 13, Issue. 3, 2019. DOI: 10.1049/iet-map.2018.5426.

[21] Bhattacharya, A., Dasgupta, B. and Jyoti. R. "Design and analysis of ultrathin X-band frequency selective surface structure for gain enhancement of hybrid antenna", *International Journal of RF and Microwave Computer-Aided Engineering*, vol. 31, Issue. 2, 2020. DOI: 10.1002/mmce.22505.

[22] Velan, S., Sundarsingh, E. F., Kanagasabai, M., Sarma, A. K., Raviteja, C., Sivasamy, R. and Pakkathillam, J. K. "Dual- Band EBG Integrated Monopole Antenna Deploying Fractal Geometry

for Wearable Applications," *IEEE Antennas and Wireless Propagation Letters*, vol.14, pp. 249-252, 2015, DOI:10.1109/LAWP.2014.2360710.

[23] Yi, X., Zhou, L., Hao, S. and Chen, X. "Dual-Band High-Gain Shared-Aperture Antenna Integrating Fabry-Perot and Reflectarray Mechanisms", *Electronics*, vol. 11, Issue. 13, 2022, DOI: 10.3390/ electronics11132017.

[24] Sah, S., Mittal, A., and Tripathy, M. R. "High gain dual band slot antenna loaded with frequency selective surface for WLAN/fixed wireless communication", *Microwave and Optical Technology Letters*, vol. 61, Issue. 2, 2018.DOI: 10.1002/ mop.31559.

[25] Chen, H. Y. and Tao, Y. "Bandwidth enhancement of a U-slot patch antenna using dual-band frequency-selective surface with double rectangular ring elements", *Microwave and Optical Technology Letters*, vol. 53, pp. 1547–1553, 2011, DOI:10.1002/mop.26066.

[26] Yang, W., Wang, H., Che, W. and Wang, J. "A Wideband and High-Gain Edge-Fed Patch Antenna and Array Using Artificial Magnetic Conductor Structures." *IEEE Antennas and Wireless Propagation Letters*, vol. 12, pp. 769-772, 2013. DOI:10.1109/LAWP. 2013.2270943.

[27] Kern, D. J., Werner, D. H., Monorchio, A., Lanuzza, L. and Wilhelm, M. J. "The design synthesis of multiband artificial magnetic conductors using high impedance frequency selective surfaces", *IEEE Transactions on Antennas and Propagation*, vol. 53, Issue. 1, 2005, DOI: 10.1109/TAP.2004.840540.

[28] Chatterjee, A., Banerjee, S., Frnda, J. and Dvorsky, M. "Planar FSS Based Dual-Band Wire Monopole Antenna for Multi-Directional Radiation With Diverse Beamwidths", *IEEE Access*, vol. 10, pp. 30427-30435, 2022, DOI: 10.1109/ACCESS.2022.3159337.

[29] Mondal, K., Bag, B., Murmu, L. *et al.* "Dual Band, Reduced Size, Enhanced Gain Frequency Selective Surface Based Monopole Antenna for Wireless Communications", *Wireless Personal Communications*, vol. 131, pp. 2797–2810, 2023. DOI: 10.1007/s11277-023-10580-4.

[30] Danuor, P., Moon, J. I. and Jung, Y. B. "High-gain printed monopole antenna with dual-band characteristics using FSS-loading and top-hat structure", *Scientific Reports*, vol. 13, 9982, 2023. DOI: 10.1038/s41598-023-37186-x.

[31] Danuor, P., Moon, J. I., Lee J. N. and Jung, Y. B. "A Pattern-Reconfigurable Antenna Using Tunable Band-Stop FSS With Reduced Switching Elements," *IEEE Antennas and Wireless Propagation Letters*, vol. 24, Issue. 1, pp. 172-176, 2025, DOI: 10.1109/LAWP.2024.3487842.

[32] Sharma , A., Khah, S. K., and Rawat, S. "Compact Y -shaped antenna with partial and meandered ground for WLAN/Wi-MAX applications," *Scientia Iranica*, vol. 31, Issue 17, pp. 1556-1566, 2024, DOI: 10.24200/sci.2022.59299.6163.

[33] Zou, Y., Kong, X., Zhou, S., Wang, L., Zhao, Y. and Gao. S. "A 3-D Wideband and High-Selectivity Amplifying Frequency-Selective Surface Based on Slot Line and Microstrip Line," *IEEE Transactions on Antennas and Propagation*, vol. 72, Issue 5, pp. 4361-4369, 2024. DOI: 10.1109/TAP.2024.3385207.

[34] Nguyen, D. D. and Seo, C. “A wideband high gain trapezoidal monopole antenna backed by frequency selective surface”, *Microwave and Optical Technology Letters*, vol. 63, Issue 9, pp. 2392-2399, 2021. DOI: 10.1002/mop.32890.

[35] Tewary, T., Maity, S., Roy, A., Mandal, K., Kundu, S. and Bhunia, S. “Design and analysis of frequency selective surface embedded broadband high gain miniaturized antenna” *International Journal of Communication Systems*, vol. 37, Issue 8, e5754, 2024. DOI: 10.1002/dac.5754.

[36] Najumunnisa, Md., Sastry, A. S. C., Madhav, B. T. P., Das, S., Hussain, N., Ali, S. S. and Aslam, M. "A metamaterial inspired AMC backed dual band antenna for ISM and RFID applications." *Sensors* vol. 22, Issue 20, 2022: 8065, DOI: 10.3390/s22208065.

[37] Panda, P. K. and Ghosh. D. "High-gain dual-band antenna with AMC surface for satellite communications." *Journal of Electromagnetic Waves and Applications* vol. 35, Issue 5, pp. 604-619, 2021: DOI: 10.1080/09205071.2020.1848641.

[38] Rajavel, V. and Ghoshal, D. "AMC-based low-profile dual-band slotted patch antenna for IoT devices in the healthcare system." *Iranian Journal of Science and Technology, Transactions of Electrical Engineering* vol. 47, Issue 2, pp. 437-450, 2023, DOI: 10.1007/s40998-022-00581-7.

[39] Garg, R., Bhartia, P., Bahl, I., Ittipiboon, A.“Microstrip Antenna Design Handbook”, Chapter 07, 1st Edition, Artech House, Norwood, 2001.

[40] Guha, D., and Antar, Y. M. M. “Microstrip and Printed Antennas: New Trends, Techniques, and Applications” Chapter 8, 1st Edition, John Wiley & Sons, Noida, India, 2011.

[41] Munk, B. A “Frequency Selective Surfaces- Theory and Design”, Chapter 02, John Wiley & Sons, 2000.

Figure 1. Geometry of the proposed CPW-fed antenna. (a) Schematic view, (b) fabricated prototype

Figure 2. Surface current distribution of the CPW-fed antenna at frequencies. (a) 2.4 GHz, (b) 5.5 GHz

Figure 3. The 3-D view of the CPW-fed antenna with the FSS-based AMC

Figure 4. Development of AMC. (a) Schematic view of unit cell, (b) simulation setup, and (c) fabricated prototype.

Figure 5. Simulated reflection phase response of the AMC for variation in stub length of cross

Figure 6. Simulated reflection phase response of the AMC for variation in loop dimension

Figure 7. Fabricated prototype of the CPW-fed antenna with the FSS-based AMC as substrate.
(a) Top-view, (b) Side view

Figure 8. Simulated and Measured reflection coefficients of the antenna with and without AMC as well as metal reflector

Figure 9. Reflection coefficients of antenna FSS-based AMC for spacing *(H)* variation

Figure 10. Simulated and measured radiation plot of antenna with and without AMC for H = 10 mm at 2.35 GHz

Figure 11. Simulated and measured radiation plot of the antenna with and without AMC for H = 10 mm at 5.5 GHz

Figure 12. The schematic diagram of the measurement setup for radiation pattern and gain of the Antenna

Figure 13. 3-D gain plot of the antenna at 2.35 GHz. (a) antenna only, (b) antenna with FSS-based AMC

Figure 14. 3-D gain plot of the antenna at 5.5 GHz. (a) antenna only, (b) antenna with FSS-based AMC

Figure 15. Three dimensional radiation plot (gain) of the antenna backed by metallic reflector (a) at 2.35 GHz; (b) at 5.5 GHz.

Table 1. Dimensions of the CPW fed Split Ring Shaped Antenna

Table 2: Dimensions of unit cell of the proposed FSS-based AMC

Table 3. Characteristics of the antenna with FSS-based AMC at H= 10 mm

Table 4. Comparison of the proposed design with other similar type antennas

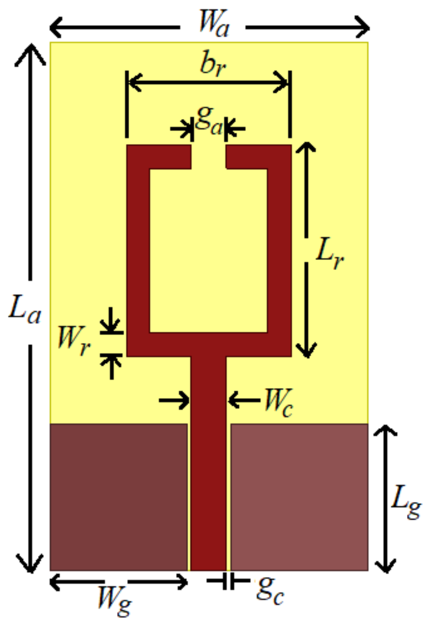

Fig. 1(a)

Fig. 1(b)

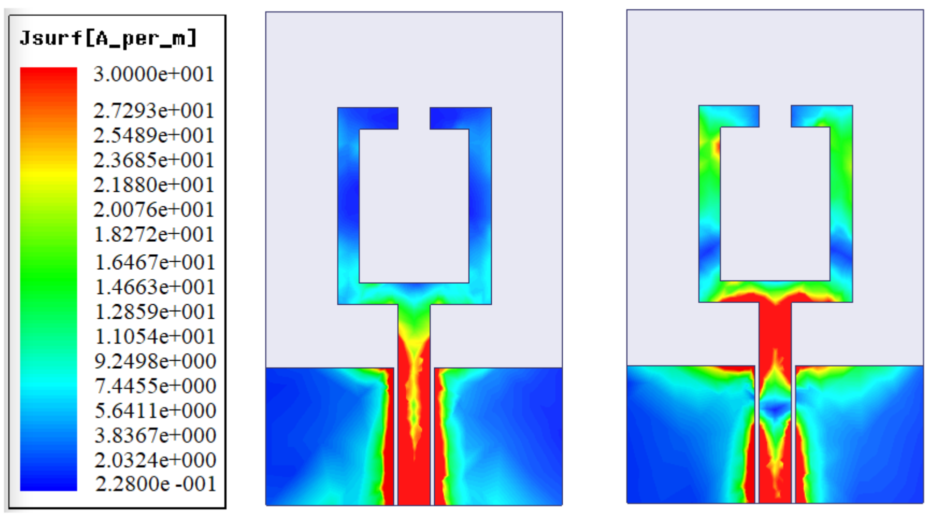

Fig. 2

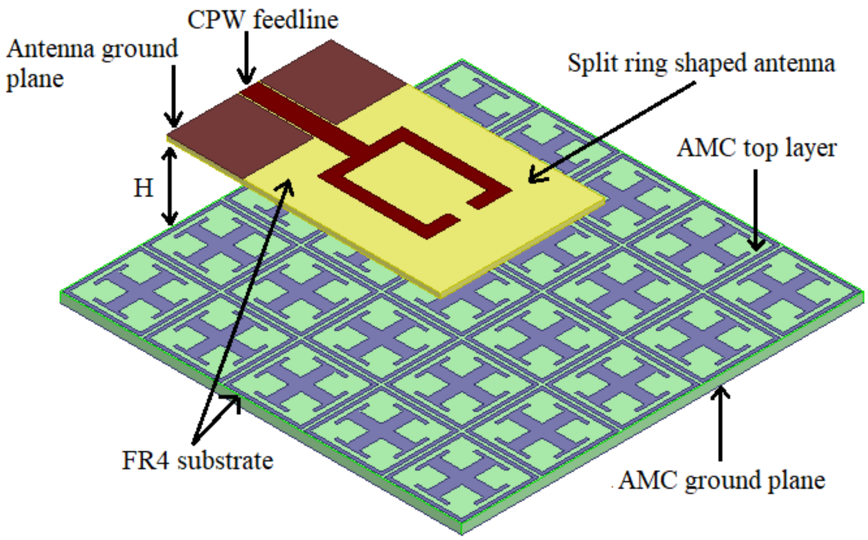

Fig. 3

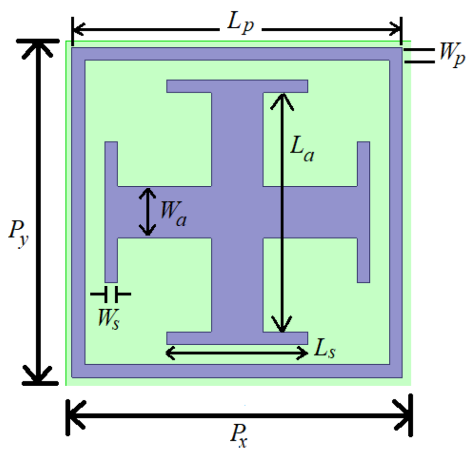

Fig. 4(a)

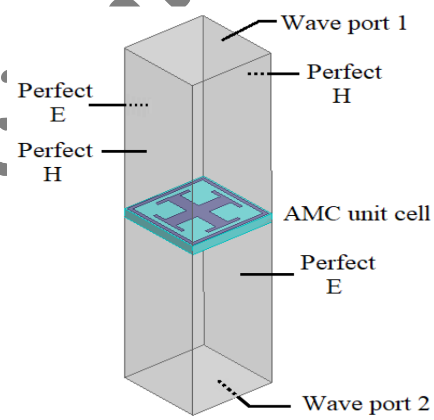

Fig. 4(b)

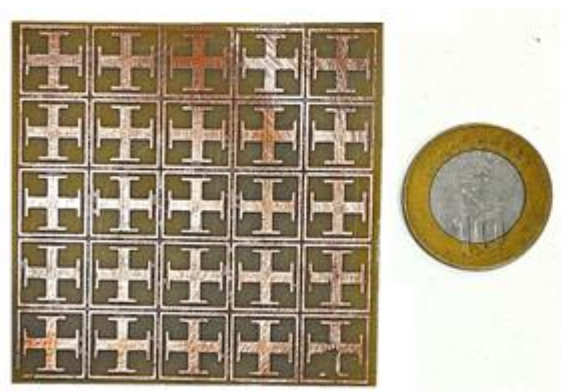

Fig. 4(c)

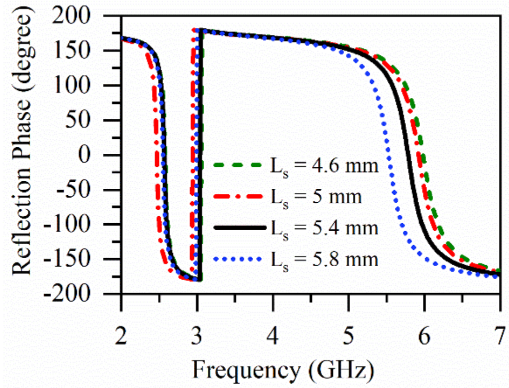

Fig. 5

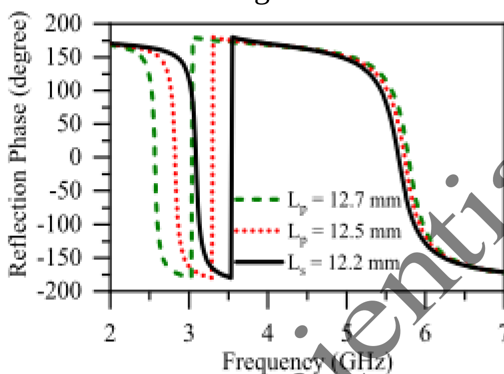

Fig. 6

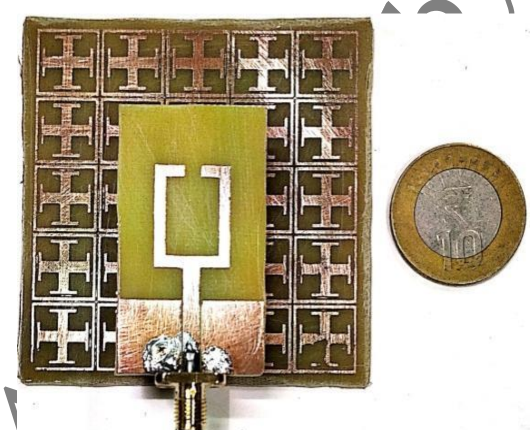
Fig. 7(a)

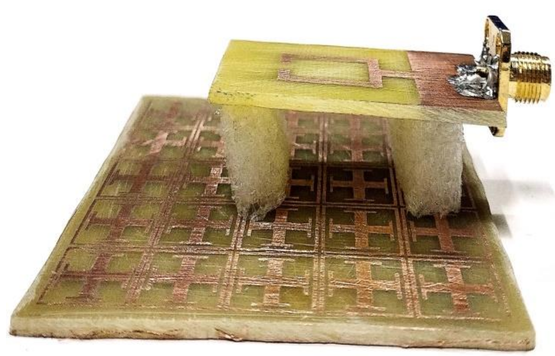
Fig. 7(b)

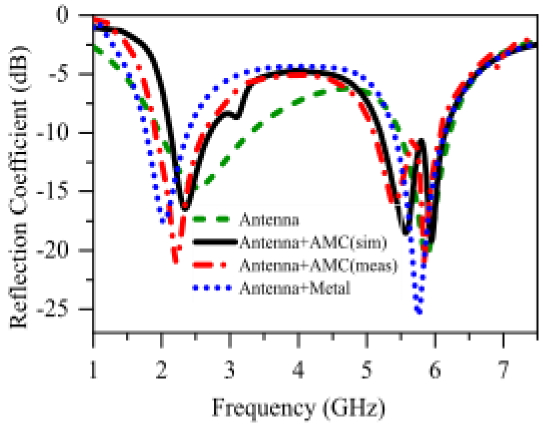

Fig. 8

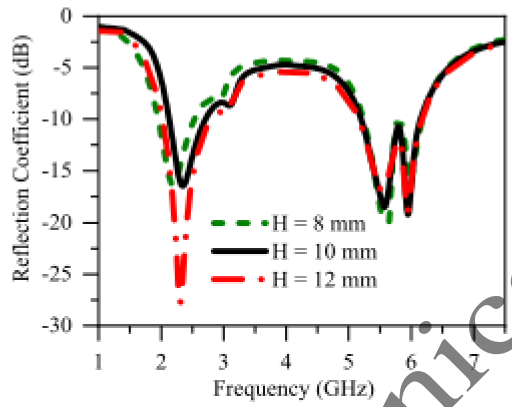

Fig. 9

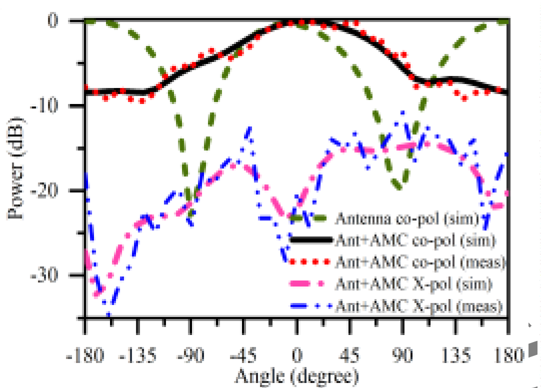

Fig. 10(a)

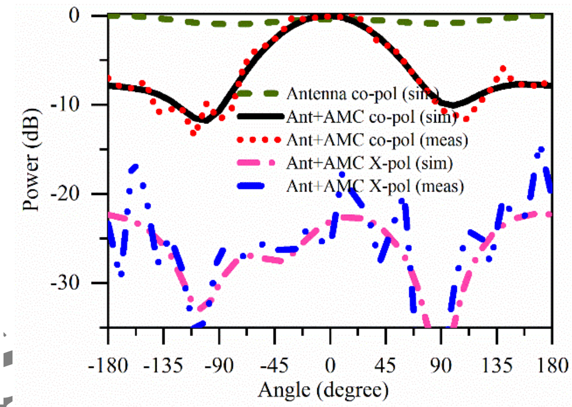

Fig. 10(b)

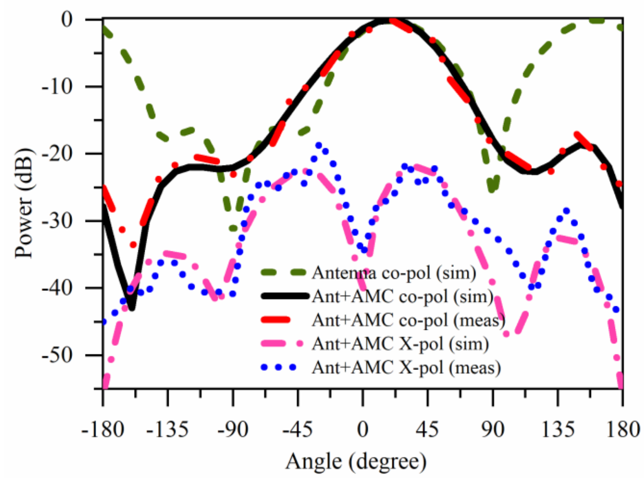

Fig. 11(a)

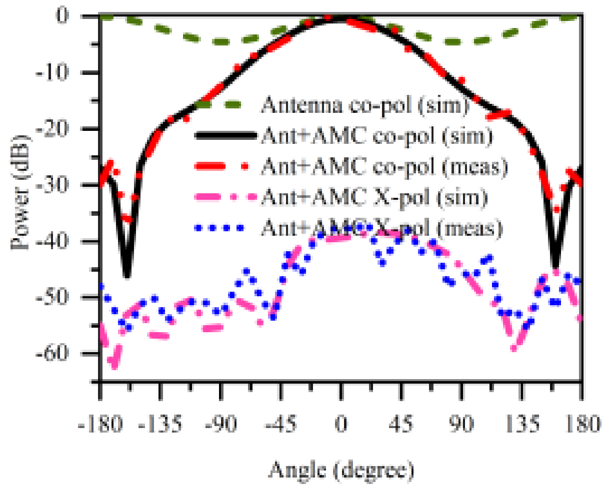

Fig. 11(b)

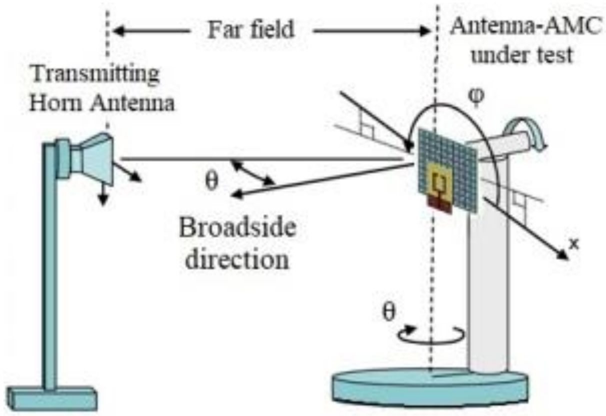

Fig. 12

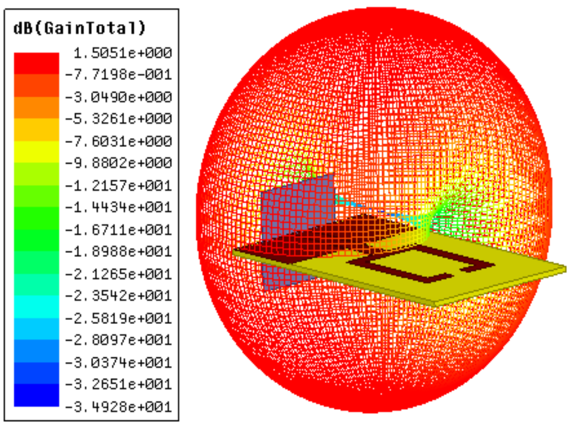

Fig. 13(a)

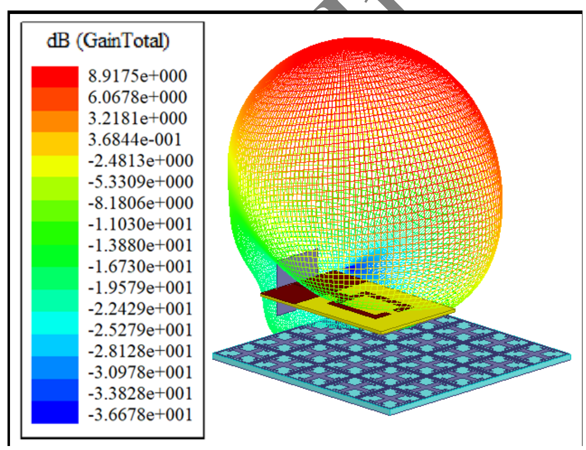

Fig. 13(b)

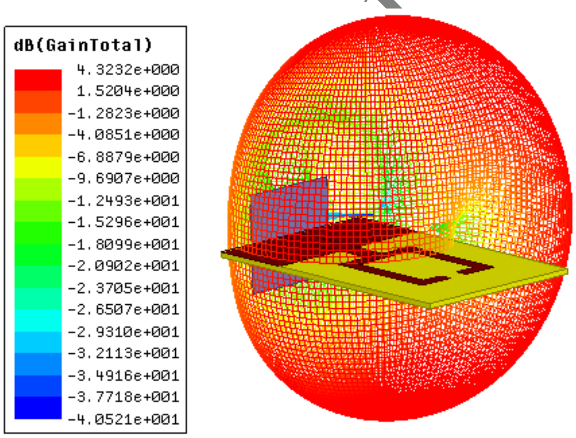

Fig. 14(a)

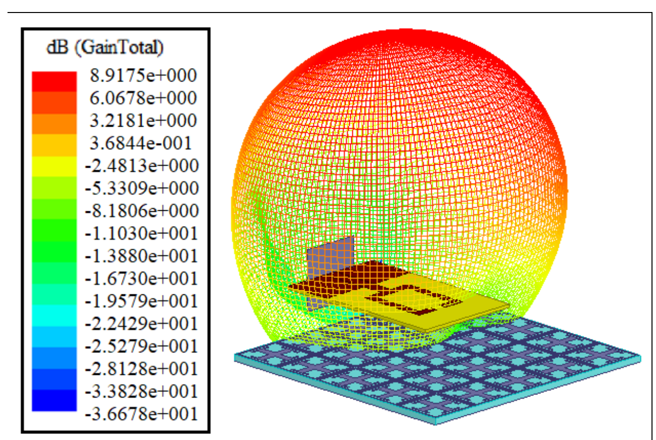

Fig. 14(b)

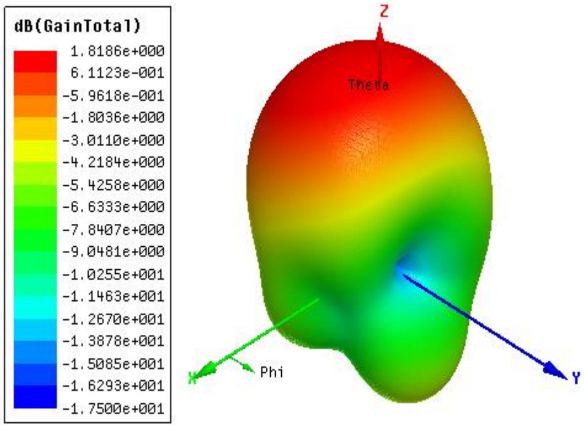

Fig. 15(a)

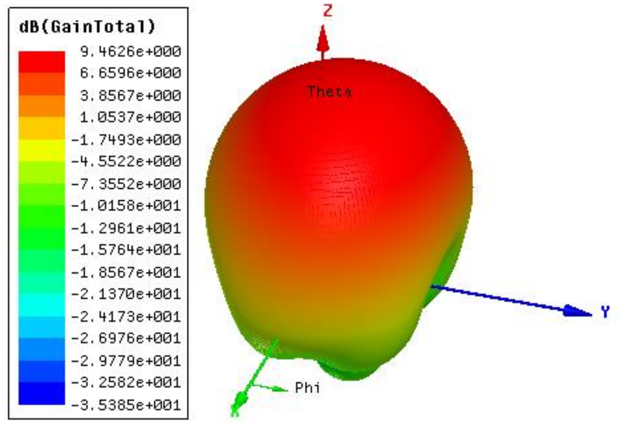

Fig. 15(b)

Table 1

Parameter	L_a	W_a	W_g	L_g	g_c	L_r	b_r	g_a	W_r	W_c
Value (mm)	45	27	11.65	12	0.35	18	14	3	2	3

Table 2

Parameter	P_x	P_y	L_p	W_p	L_a	L_s	W_a	W_s
Value (mm)	13.2	13.2	12.7	0.5	9.2	5.4	2	0.5

Table 3

Parameter (Frequency in GHz)	F/B ratio (dB)		Peak gain (dBi)	
	2.35	5.5	2.35	5.5
Antenna	0.51	4.37	1.5	4.3
Antenna + FSS (simulated)	8.45	14.8	8.5	8.92
Antenna + FSS (measured)	8.1	14.1	8.2	8.6

Table 4

Antenna Parameter	**Ref [13]**	**Ref [18]**	**Proposed**
Antenna	Wideband	Dualband	Dualband
Frequency band (GHz)	3.3-17.85	2.48 / 5.72	2.4 / 5.8
-10 dB bandwidth	138%	7% / 17.8%	25% / 18%
Number of layers	1	2	2
Layer spacing	---	12 ($0.2\lambda_0$)	10 ($<0.25\lambda_0$)
Unit cell (mm)	13x13	16x16	13.2 x 13.2 ($0.1\lambda_0$)
Gain (dBi)	4.45	7.54 / 6.8	8.5 / 8.92
Angular stability	30^0	---	90^0
Reflection phase	----	----	Linear
Technology used	Fractal	Cascading	Cascading

Brief technical biography of authors

Dr. Sujit Goswami Dr. Sujit Goswami received M. Tech in Telecommunication Engineering from National Institute of Technology, Durgapur in 2010. He obtained PhD in Electronics and Communication Engineering from National Institute of Technology, Durgapur in the year 2025. From 2007 to 2010 he worked as a Lecturer in the Department of ECE at Asansol Engineering College, West Bengal. Presently he is working as an Assistant Professor in the Department of ECE at Asansol Engineering College, West Bengal. His research interests include multiband and wideband printed antenna design for wireless communications. He received the Visvesvaraya Part-time PhD fellowship under the Ministry of Electronics and Information Technology (MeitY), Govt of India, under the Visvesvaraya Ph.D scheme. He is a Member of The Institution of Engineers (India) and The Indian Society for Technical Education (ISTE).

Sujit Kumar Mandal received B. Sc degree in Physics (H) from University of Calcutta in 2001. He completed B. Tech and M. Tech in Radio Physics & Electronics from Institute of Radio Physics & Electronics, C. U. in the year 2004 and 2006 respectively. He received Ph.D. degree from National Institute of Technology, Durgapur wherein he is an Assistant Professor in the Department of Electronics and Communication Engineering, since 2010.

His present research area includes the application of soft computing techniques, artificial intelligence, machine learning, and deep learning algorithms in antenna arrays, Direction of Arrival (DoA) Estimation, time-modulated antenna arrays, RF energy harvesting, and on-chip antenna design. He has published more than 60 research papers in different peer reviewed National and International journals and conferences.

SOUMEN BANERJEE (Senior Member, IEEE) received his B.Sc. (Hons.) degree in Physics from the University of Calcutta in 1998, followed by B.Tech. and M.Tech. degrees in Radio Physics and Electronics from the same University of Calcutta in 2001 and 2003, respectively. He earned his Ph.D. degree in Engineering from Indian Institute of Engineering Science and Technology (IIEST), Shibpur, India. He has served as a Visiting Faculty at the Department of Applied Physics, University of Calcutta, and is currently the Principal of Narula Institute of Technology, Agarpara, Kolkata, West Bengal, India. With over 20 years of teaching and research experience, Dr. Banerjee has authored numerous books and book chapters in the fields of communication engineering, electromagnetic field theory, microwaves, and antennas. He has also edited three books published by Springer.

His research interests include wide band gap semiconductor-based IMPATT diodes, SIW-based and printed antennas and arrays, Frequency Selective Surfaces (FSS), Dielectric Resonator Antennas, Body-wearable antennas, and the applications of Artificial Intelligence, Machine Learning and Computer Vision. Dr. Banerjee has published more than 100 research papers in International journals and conferences. He is a Senior Member of the IEEE Antennas and Propagation (AP) and Microwave Theory and Techniques (MTT) Societies, a Fellow of the IETE

(New Delhi), and a Life Member of the Indian Radio Science Society (InRaSS). He is a regular reviewer for several reputed International journals published by IEEE, Springer, Taylor & Francis, Wiley, and others. He has also served as Conference Chair and technical session chair in numerous International conferences.

Dr. Ayan Chatterjee Dr. Ayan Chatterjee received M.Tech in Communication Engineering from University of Kalyani in 2012. He obtained PhD in Microwave Engineering from Indian Institute of Engineering Science and Technology (IIEST), Shibpur in the year 2018. From 2012 to 2013 he worked as Assistant Professor in the Department of ECE at SKFGI, West Bengal. From 2018 to 2021 he served the Department of ECE at National Institute of Technology, Sikkim. Presently he is working as an Associate Professor in the Department of ECE at University of Engineering and Management, Kolkata. He has authored and co-authored more than 60 papers in referred journals and conference proceedings. His research interests include Planar and Non-planar Frequency Selective Surfaces, Metamaterial Inspired Surfaces, Wideband Antennas and Antennas for Wearable Technology. He received Senior Research Fellowship from CSIR, Government of India in 2014. He has received Research Grant from DST-SERB in 2023 under SURE sceme. Dr. Chatterjee is actively volunteering several reputed journals such as IEEE Transactions on Antennas and Propagation, IEEE Transactions on Microwave Theory and Technology, IEEE Access, IEEE AWPL, Journal of Electromagnetic Waves and Applications, and many more. He is a Senior Member of URSI as well as IEEE and a Member of Institution of Engineers (India). He is also serving IEEE as an Exe-com Member of the AP/MTT Kolkata Chapter.